

Supplementary Figure 1. Microbiome analysis in 3xTg mouse stool reveals an age-dependent alteration in the microbial community.

(A) Relative abundance of bacterial phyla determined by high throughput sequencing analysis (n=5).

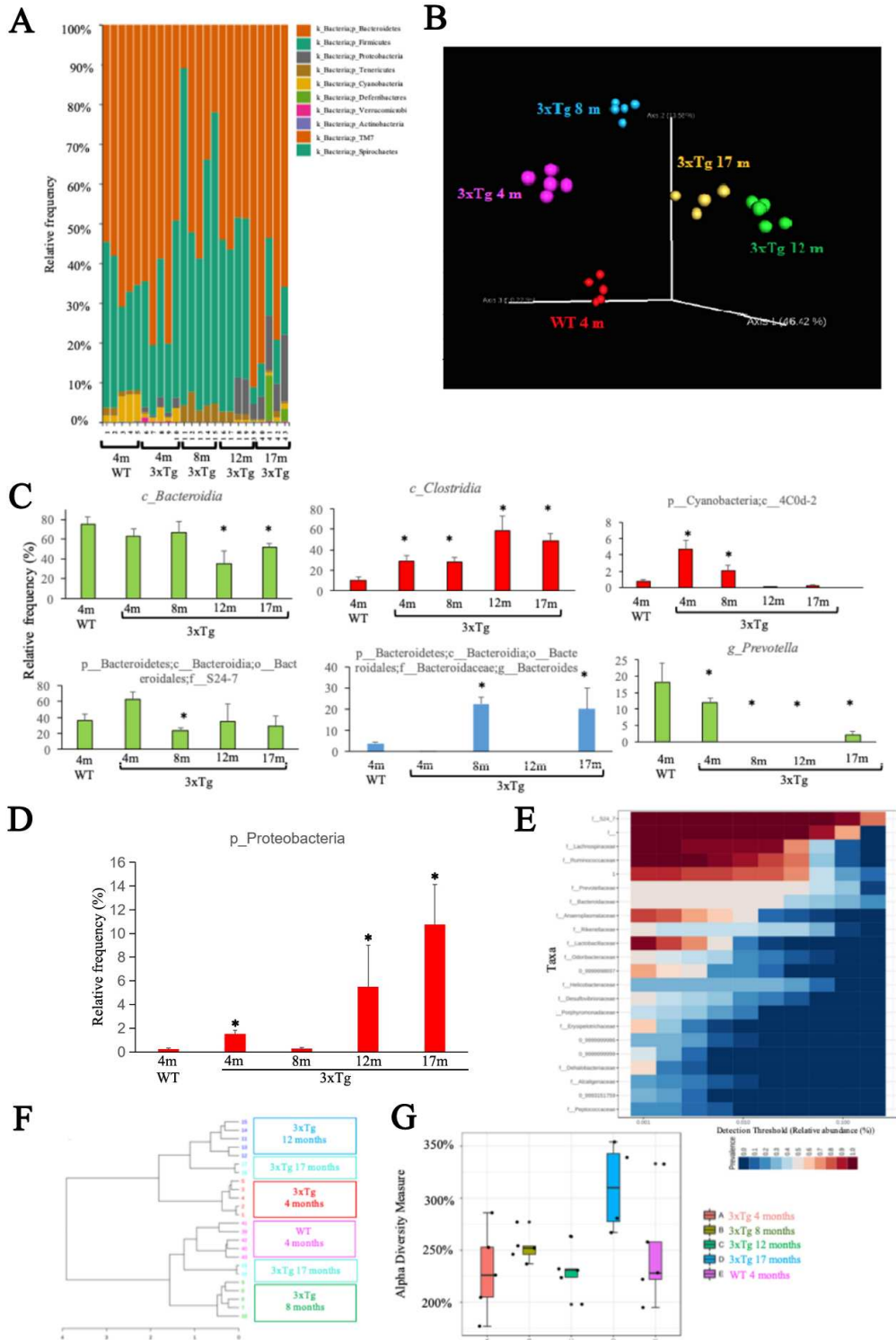
(B) Principal coordinate plot (PCoA) of microbial community structure in an age-dependent manner in 3xTg and WT mouse stool.

(C) Mean relative frequency of bacterial species. Data represent the means \pm SEM; *P < 0.05 compared with control (WT 4 months), one-way ANOVA.

(D) Mean relative frequency of proteobacterial phylum. Data represent the means \pm SEM; *P < 0.05 compared with control (WT 4 months), one-way ANOVA.

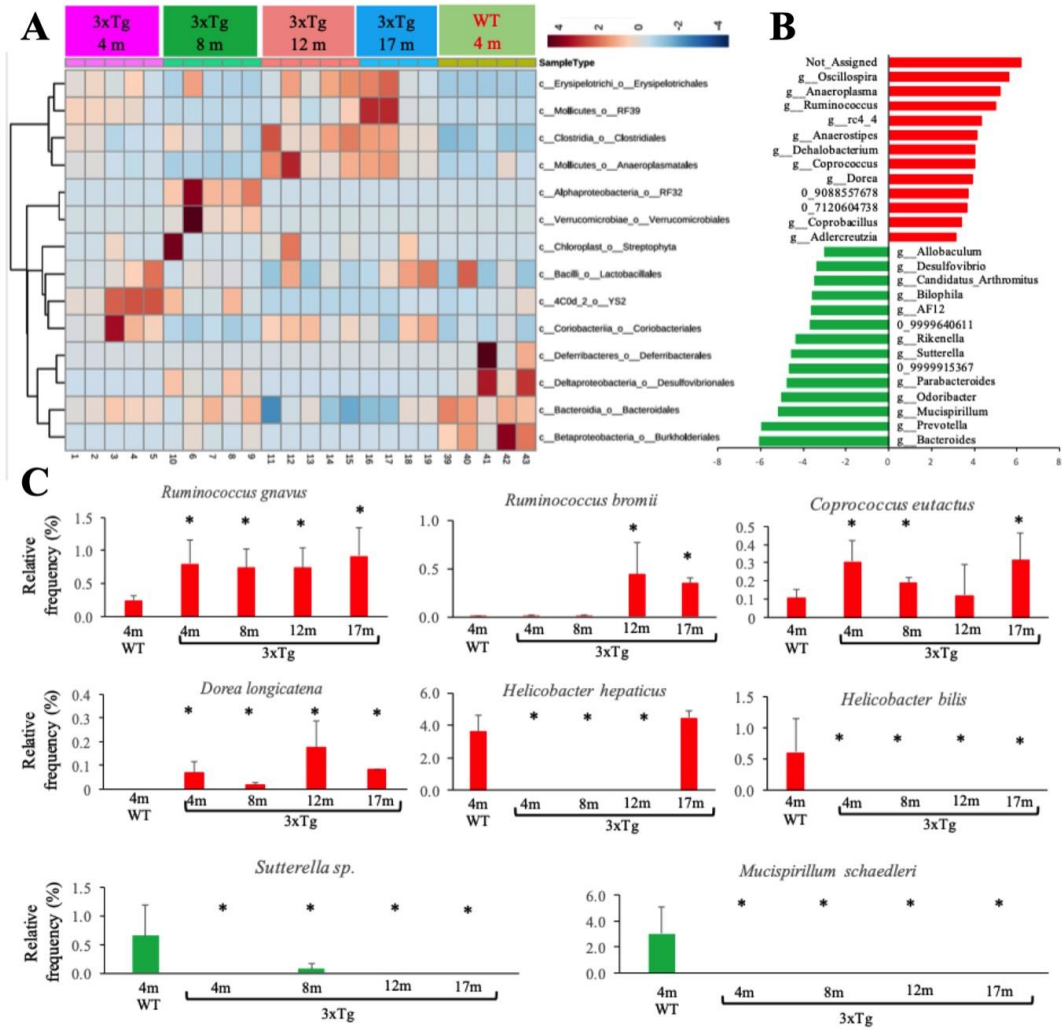
(E and F) Hierarchical clustering of the core microbial taxa shows alterations of abundances across different age groups of 3xTg and WT mouse.

(G) Boxplot of α -diversity pattern (Chao1) of the microbiota across different age groups in the 3xTg and WT mouse stool.



Supplementary Figure 2. Comparative and biomarker discovery analysis using relative taxonomic abundances reveal microbiome disequilibrium between 3xTg and wild-type mouse stool.

- (A) Hierarchical clustering and heatmap analysis using taxonomic abundances.
- (B) Biomarker analysis of the microbial genera in 3xTg and WT mouse stool.
- (C) Mean relative abundance of bacterial phyla determined by high-throughput sequencing analysis (n = 5).



Supplementary Figure 3. Characterization of Germ-free 3xTg mice

(A) Body weights of Germ-free 3xTg mice and SPF 3xTg mice at the age of 7.5 months.

Data represent the mean \pm SEM; representative data of eight samples; **P < 0.01 compared with control, unpaired t tests.

(B) Representative pictures of cecum from Germ-free 3xTg mice and SPF 3xTg mice. Germ-free 3xTg mice have enlarged cecum compared with SPF 3xTg mice.

(C) Representative pictures of gastrointestinal tract from both male and female Germ-free 3xTg mice and SPF 3xTg mice.

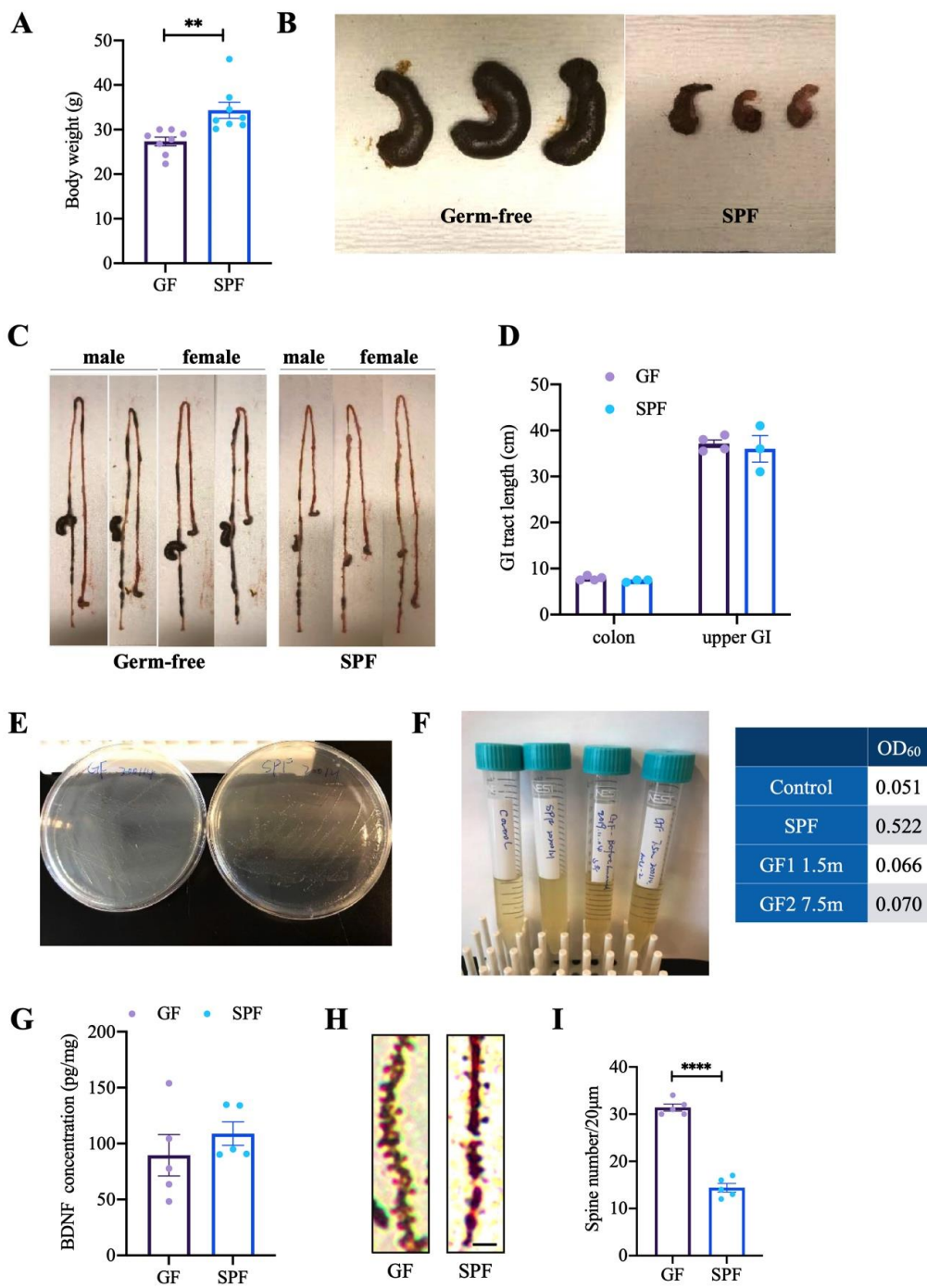
(D) Quantification analysis of gastrointestinal tract length from Germ-free 3xTg mice and SPF 3xTg mice. Data represent the mean \pm SEM; representative data of three to four samples, unpaired t tests.

(E&F) *In vitro* culture of bacteria from fecal pellets of Germ-free 3xTg mice and SPF 3xTg mice

(G) BDNF concentrations in the brains of Germ-free 3xTg mice and SPF 3xTg mice. Data represent the mean \pm SEM; representative data of five samples; unpaired t tests.

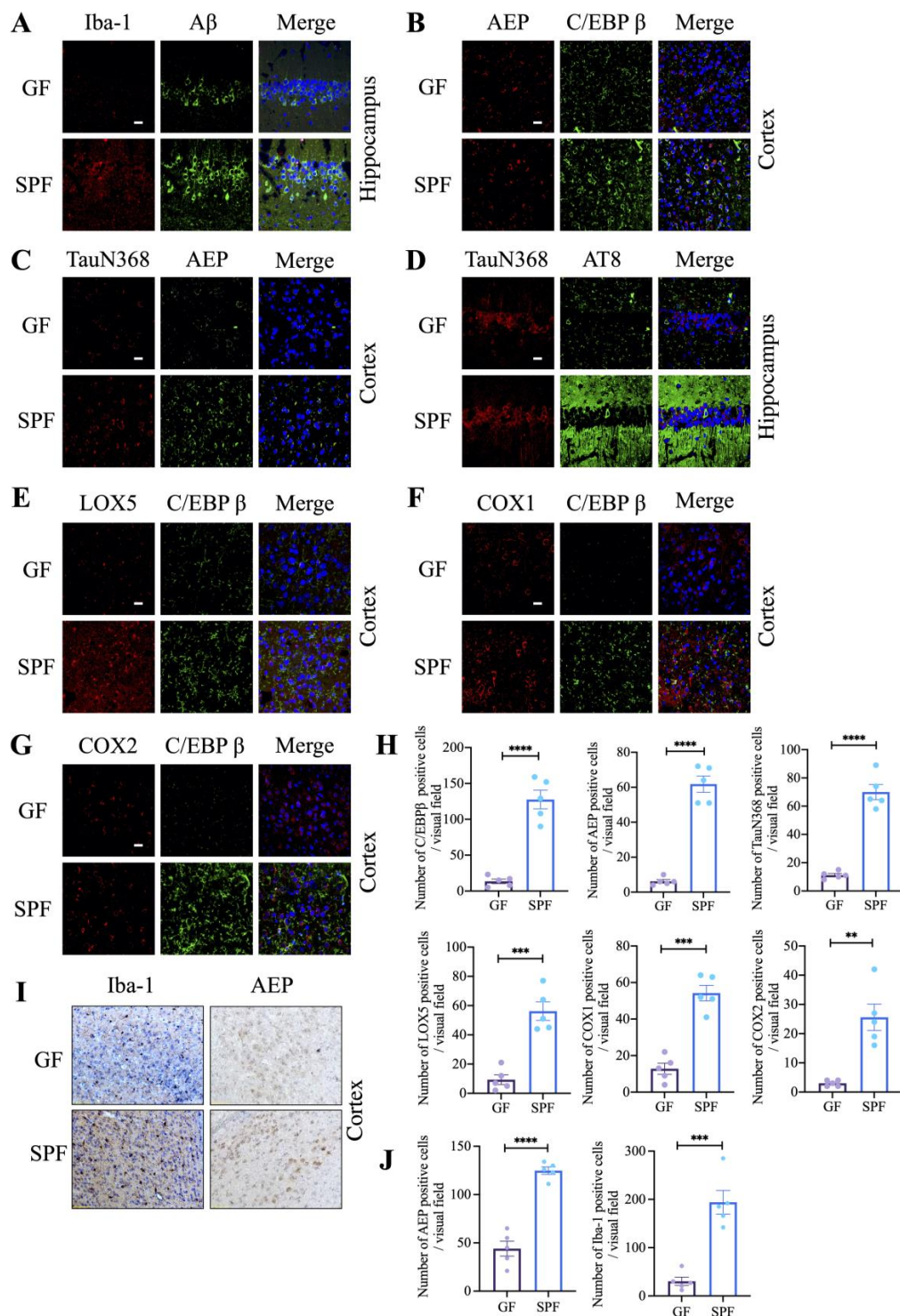
(H) The dendritic spines from the apical dendritic layer of the hippocampus region were analyzed by Golgi staining. Scale bar: 5 μ m.

(I) Quantitative analysis of the spine density. (n = 5 in each group, Data are shown as mean \pm SEM. ****P < 0.0001).

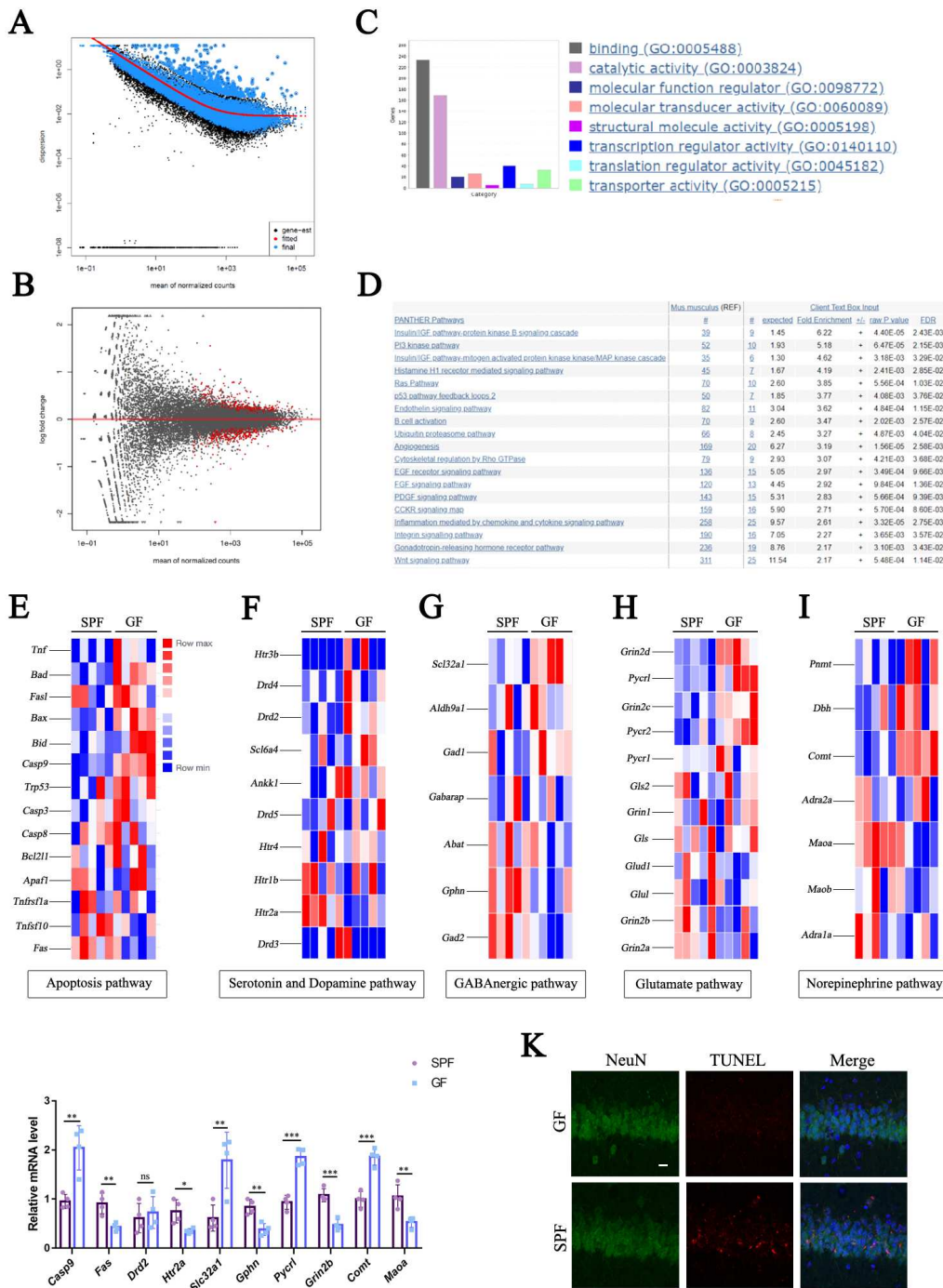


Supplementary Figure 4. Germ-free 3xTg mice exhibit diminished AD pathologies and AA-associated inflammation.

- (A) Immunofluorescent staining of Iba-1 (red) and A β (green) in the hippocampus CA1 region of the brains from Germ-free 3xTg mice and SPF 3xTg mice. Scale bar: 20 μ m.
- (B) Immunofluorescent staining of AEP (red) and C/EBP β (green) in the cortex region of the brains from Germ-free 3xTg mice and SPF 3xTg mice. Scale bar: 20 μ m.
- (C) Immunofluorescent staining of TauN368 (red) and AEP (green) in the cortex region of the brains from Germ-free 3xTg mice and SPF 3xTg mice. Scale bar: 20 μ m.
- (D) Immunofluorescent staining of TauN368 (red) and AT8 (green) in the hippocampus CA1 region of the brains from Germ-free 3xTg mice and SPF 3xTg mice. Scale bar: 20 μ m.
- (E) Immunofluorescent staining of LOX5 (red) and C/EBP β (green) in the cortex region of the brains from Germ-free 3xTg mice and SPF 3xTg mice. Scale bar: 20 μ m.
- (F) Immunofluorescent staining of COX1 (red) and C/EBP β (green) in the cortex region of the brains from Germ-free 3xTg mice and SPF 3xTg mice. Scale bar: 20 μ m.
- (G) Immunofluorescent staining of COX2 (red) and C/EBP β (green) in the cortex region of the brains from Germ-free 3xTg mice and SPF 3xTg mice. Scale bar: 20 μ m.
- (H) Quantitative analysis of C/EBP β positive cells, AEP positive cells, TauN368 positive cells, LOX5 positive cells, COX1 positive cells, and COX2 positive cells, respectively. The densities of C/EBP β , AEP, TauN368, LOX5, COX1 and COX2 positive cells were significantly increased in SPF 3xTg mice brain. Hippocampus: A and D; Cortex: B, C, E, F and G. (n = 5 in each group, Data are shown as mean \pm SEM. **P < 0.01, ***P < 0.001, ****P < 0.0001 compared with control, unpaired t tests).
- (I) Immunohistochemistry staining of Iba-1 and AEP in the cortex region of the brains from Germ-free 3xTg mice and SPF 3xTg mice.



(J) Quantitative analysis of AEP positive cells and Iba-1 positive cells in mice cortex. The densities of AEP, and Iba-1 positive cells were significantly increased in SPF 3xTg mice brain. (n = 5 in each group, Data are shown as mean \pm SEM. ***P < 0.001, ****P < 0.0001 compared with control, unpaired t tests).



Supplementary Figure 5. Summary of transcriptome sequencing results of mRNA expression in the hippocampal samples from germ-free and SPF 3xTg mice.

(A) Dispersion plot showing empirical (black dots) and fitted (red lines) dispersion values plotted against the mean of normalized counts.

(B) MA-plot of normalized mean versus log₂ fold change for the contrast Germ-free versus SPF 3xTg mice.

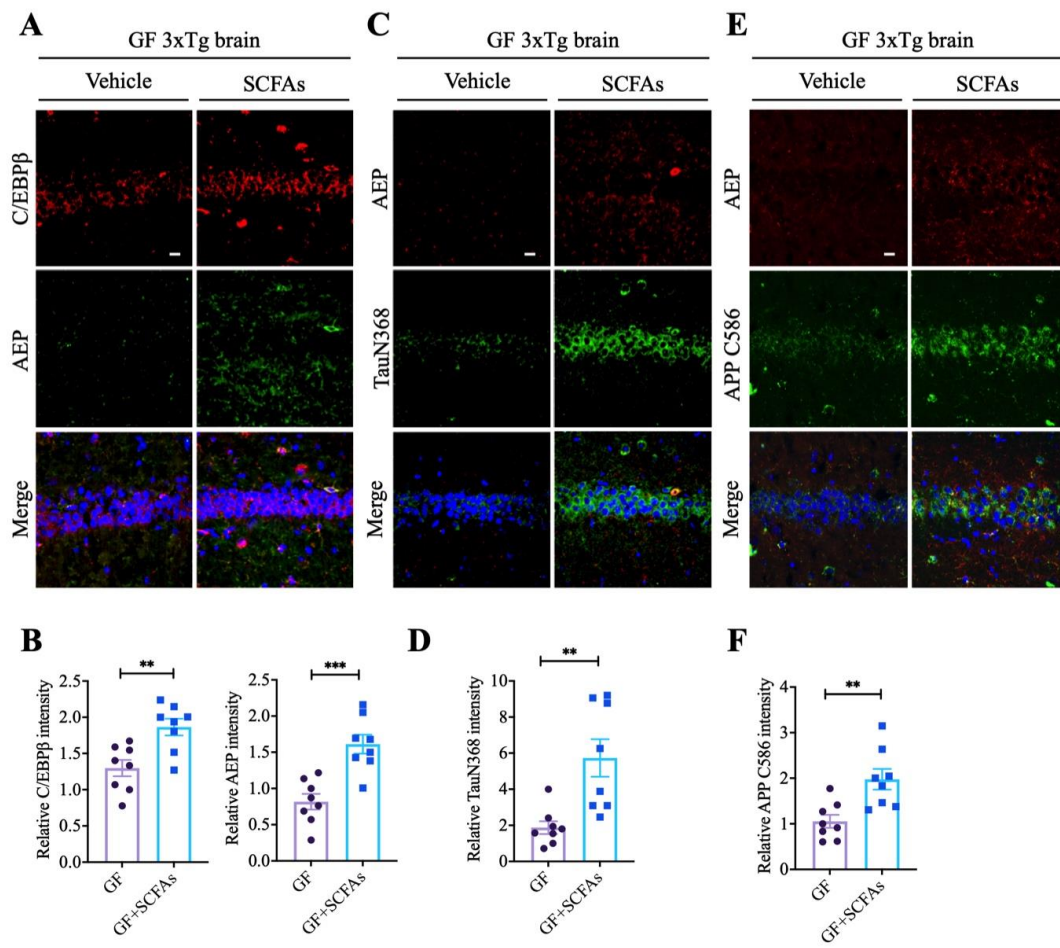
(C) PANTHER pathway analysis of differential genes.

(D) Table showing PANTHER analysis of enriched pathways.

(E-I) Heatmap showing differential genes of apoptotic, serotonin and dopamine, GABAergic, glutamate, and norepinephrine pathways.

(J) qRT-PCR analysis of representative genes in apoptotic, serotonin and dopamine, GABAergic, glutamate, and norepinephrine pathways.

(K) Immunofluorescent staining of NeuN (green) and TUNEL (red) in the hippocampus CA1 region of the brains from Germ-free 3xTg mice and SPF 3xTg mice. Scale bar: 20 μ m.



Supplementary Figure 6. SCFAs stimulate AD pathologies in Germ-free 3xTg mice.

(A) Immunofluorescent staining of C/EBP β (red) and AEP (green) in the hippocampus CA1 region of the brains from vehicle treated Germ-free 3xTg mice and SCFAs treated Germ-free 3xTg mice. Scale bar: 20 μ m.

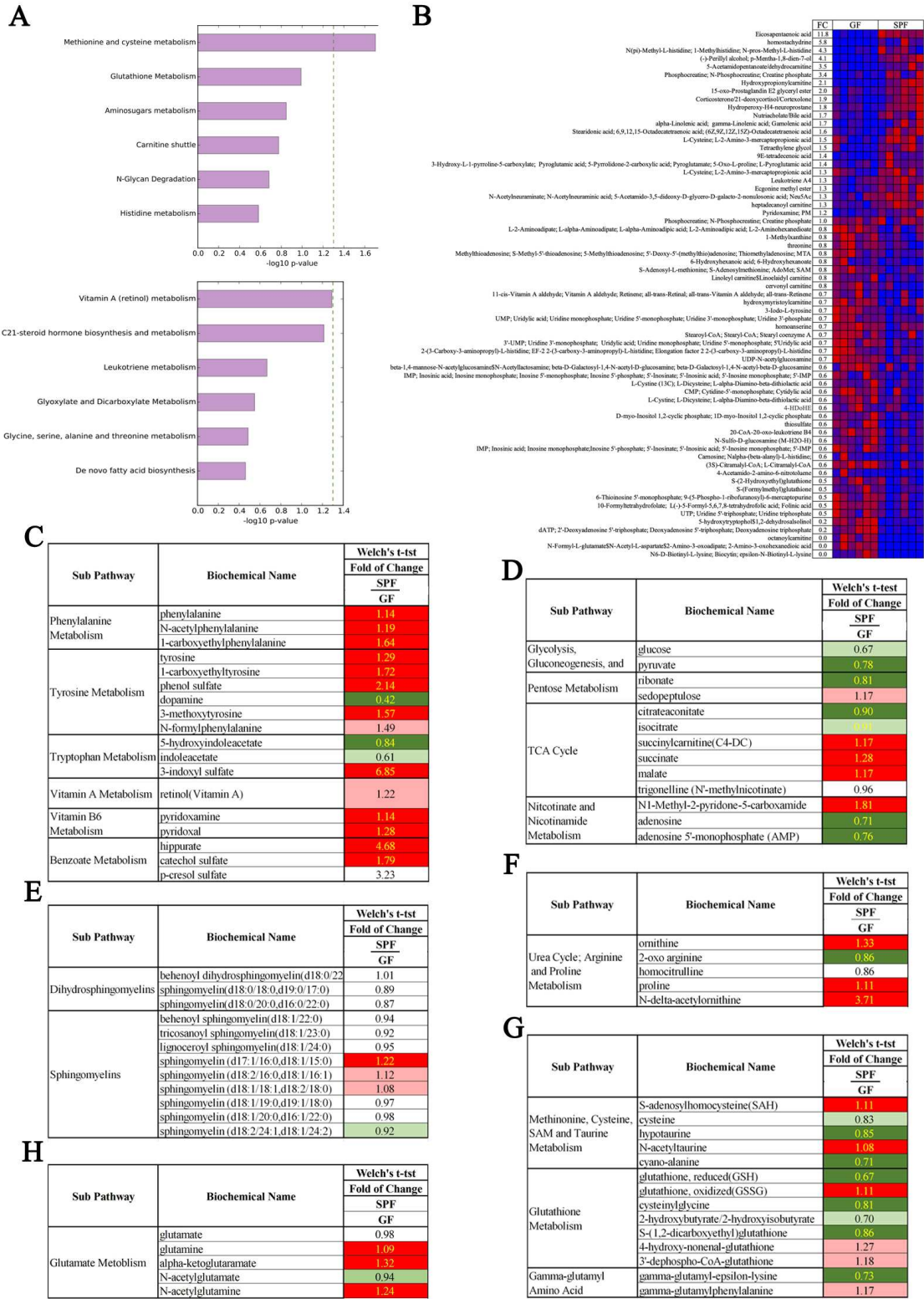
(B) Quantitative analysis of C/EBP β positive cells and AEP positive cells. The fluorescence intensity of C/EBP β positive cells and AEP positive cells in the brain of Germ-free 3xTg mice increased with SCFAs treatment. (n = 8 in each group, Data are shown as mean \pm SEM. **P < 0.01, ***P < 0.001 compared with control, unpaired t tests)

(C) Immunofluorescent staining of AEP (red) and TauN368 (green) in the hippocampus CA1 region of the brains from vehicle-treated Germ-free 3xTg mice and SCFAs-treated Germ-free 3xTg mice. Scale bar: 20 μ m.

(D) Quantitative analysis of TauN368 positive cells. The fluorescence intensity of TauN368 positive cells in the brain of Germ-free 3xTg mice increased with SCFAs treatment. (n = 8 in each group, Data are shown as mean \pm SEM. **P < 0.01 compared with control, unpaired t tests)

(E) Immunofluorescent staining of AEP (red) and APPC586 (green) in the hippocampus CA1 region of the brains from vehicle-treated Germ-free 3xTg mice and SCFAs-treated Germ-free 3xTg mice. Scale bar: 20 μ m.

(F) Quantitative analysis of APPC586 positive cells. The fluorescence intensity of APPC586 positive cells in the brain of Germ-free 3xTg mice increased with SCFAs treatment. (n = 8 in each group, Data are shown as mean \pm SEM. **P < 0.01 compared with control, unpaired t tests)



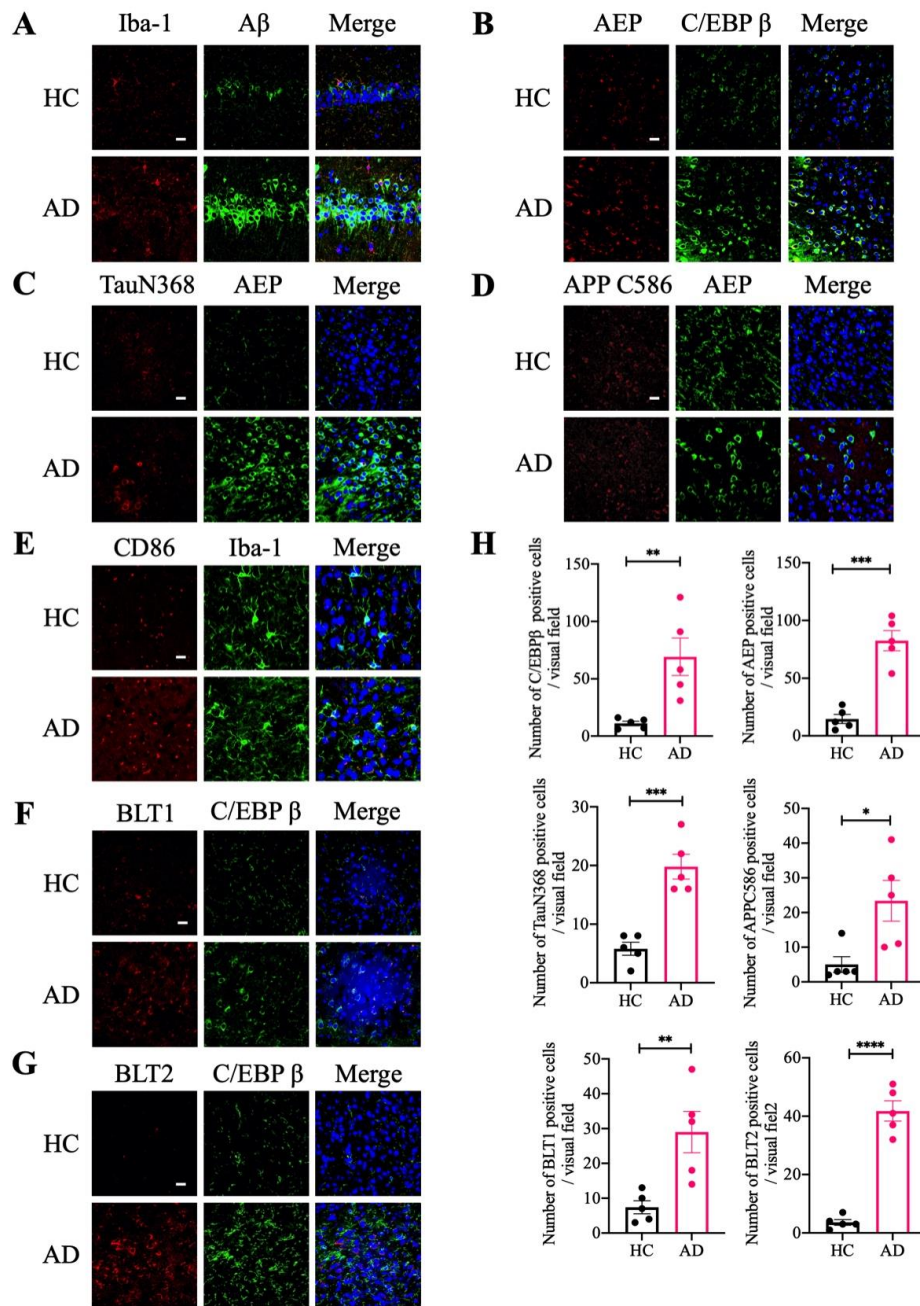
Supplementary Figure 7. Metabolomics analysis of the brains from Germ-free and SPF 3xTg mice.

(A) Differential metabolism pathway in brains from Germ-free 3xTg mice versus SPF 3xTg mice.

(B) Heatmap showing differential metabolites in Germ-free 3xTg mice versus SPF 3xTg mice.

(C-H) Metabolomics analysis of the brains from SPF versus GF 3xTg mice. The differences in microbiomes related metabolites from amino acids (C); carbohydrate and energy (D); lipids (E); arginine (F); oxidative stress (G) and glutamate metabolism (H).

(Red and green shaded cells indicate $p \leq 0.05$ (red indicates the fold change values are significantly higher for that comparison; green values significantly lower). Light red and light green shaded cells indicate $0.05 < p < 0.10$ (light red indicates the fold change values trend higher for that comparison; light green values trend lower)).



Supplementary Figure 8. AD fecal humanized ex-Germ-free mice exhibit augmented AD pathologies and escalated inflammatory AA metabolic genes.

(A) Immunofluorescent staining of Iba-1 (red) and A β (green) in the hippocampus CA1 region of the brains from HC humanized ex-GF 3xTg mice and AD humanized ex-GF 3xTg mice. Scale bar: 20 μ m.

(B) Immunofluorescent staining of AEP (red) and C/EBP β (green) in the cortex region of brains from HC humanized ex-GF 3xTg mice and AD humanized ex-GF 3xTg mice. Scale bar: 20 μ m.

(C) Immunofluorescent staining of TauN368 (red) and AEP (green) in the cortex region of the brains from HC and AD humanized ex-GF 3xTg mice. Scale bar: 20 μ m.

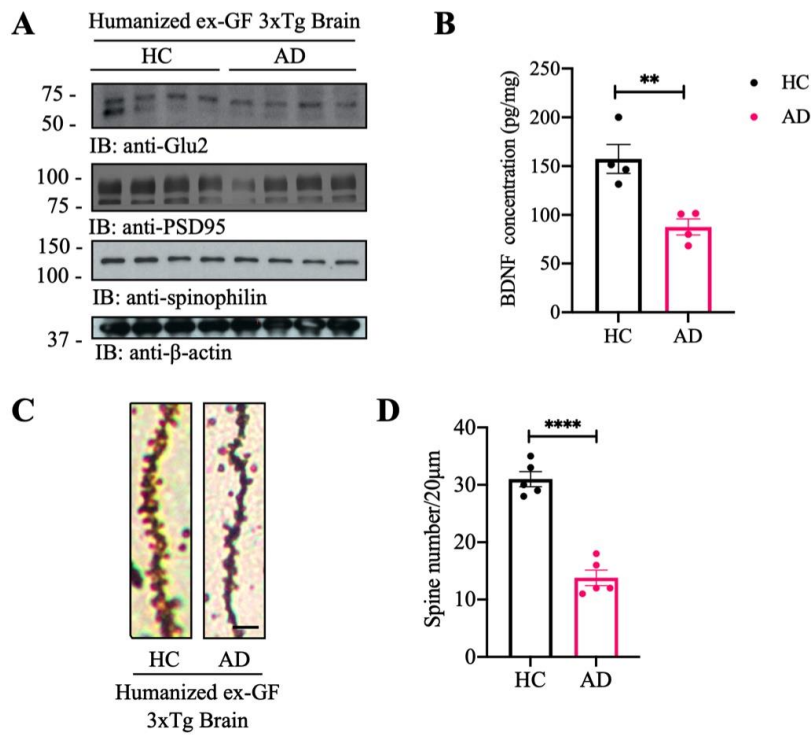
(D) Immunofluorescent staining of APPC586 (red) and AEP (green) in the cortex region of the brains from HC humanized and AD humanized ex-GF 3xTg mice. Scale bar: 20 μ m.

(E) Immunofluorescent staining of CD86 (red) and Iba-1 (green) in the cortex region of the brains from HC and AD humanized ex-GF 3xTg mice. Scale bar: 20 μ m.

(F) Immunofluorescent staining of BLT1 (red) and C/EBP β (green) in the cortex region of the brains from HC and AD humanized ex-GF 3xTg mice. Scale bar: 20 μ m.

(G) Immunofluorescent staining of BLT2 (red) and C/EBP β (green) in the cortex region of brains from HC and AD humanized ex-GF 3xTg mice. Scale bar: 20 μ m.

(H) Quantitative analysis of C/EBP β positive cells, AEP positive cells, TauN368 positive cells, APPC586 positive cells, BLT1 positive cells, and BLT2 positive cells, respectively. The densities of C/EBP β , AEP, TauN368, APPC586, BLT1 and BLT2 positive cells were significantly increased in AD humanized ex-GF 3xTg mice brains. (n = 5 in each group, Data are shown as mean \pm SEM. *P < 0.05, **P < 0.01, ***P < 0.001, ****P < 0.0001 compared with control, unpaired t tests).



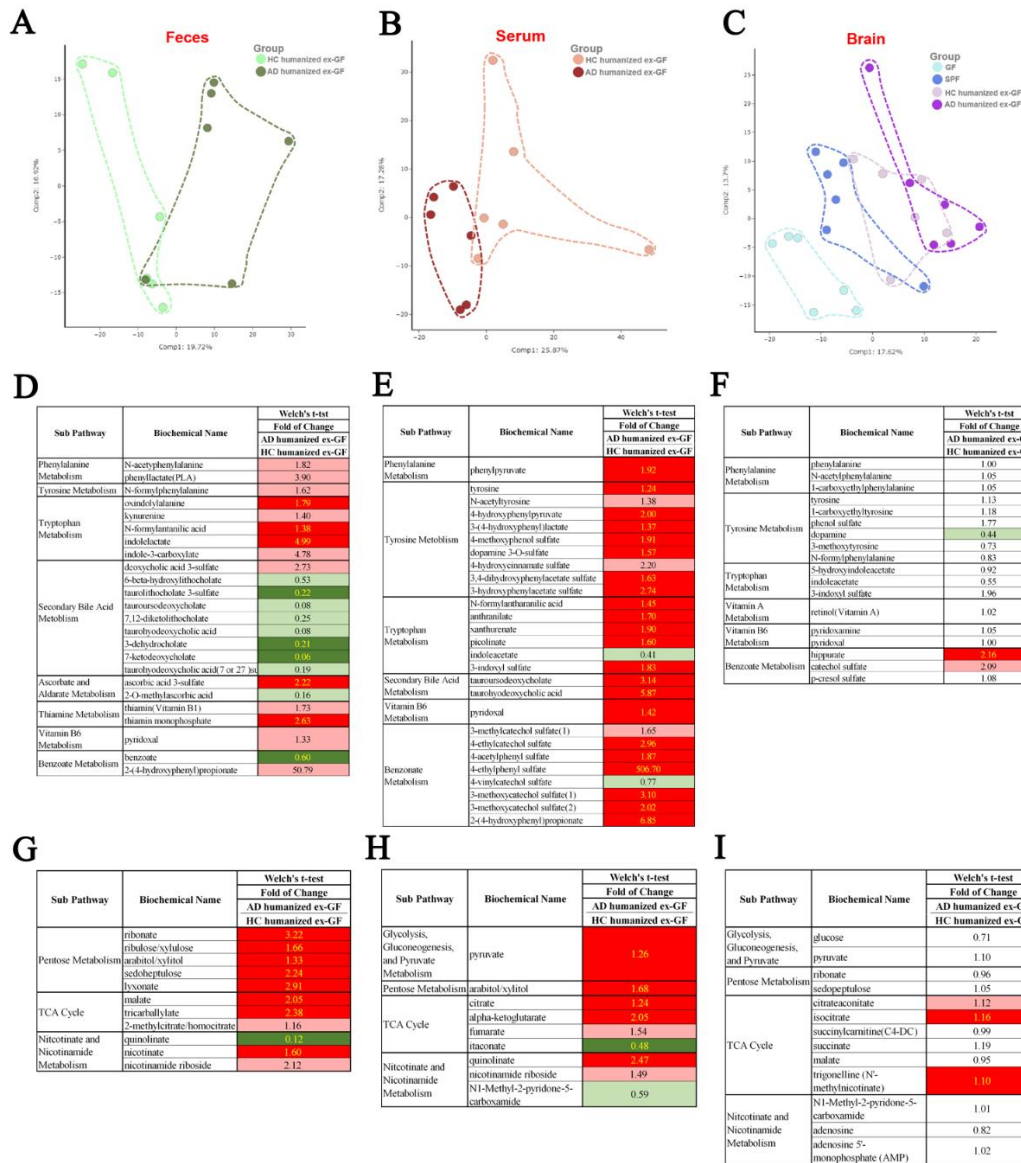
Supplementary Figure 9. AD patient gut microbiome humanized ex-Germ-free mice decrease dendritic spines and synaptic proteins.

(A) Immunoblotting analysis of synaptic markers in the brain homogenates from HC and AD humanized ex-GF 3xTg mice. The expression of synaptic markers decreased in AD humanized ex-GF 3xTg mice.

(B) BDNF concentrations in the brains of HC and AD humanized ex-GF 3xTg mice. Data represent the mean \pm SEM; representative data of four samples; unpaired t tests.

(C) The dendritic spines from the apical dendritic layer of the hippocampus region were analyzed by Golgi staining. Scale bar: 5 μ m.

(D) Quantitative analysis of the spine density. (n = 5 in each group, Data are shown as mean \pm SEM. ****P < 0.0001).



Supplementary Figure 10. Metabolomics analysis of the brains, serum samples and feces from HC humanized ex-GF 3xTg mice and HC humanized ex-GF 3xTg mice, and the brains from SPF versus GF mice.

(A-C) Principal Component Analysis (PCA). PCA of feces and serum dataset from AD and HC humanized ex-GF groups (A&B). Within the feces dataset, the HC humanized ex-GF group segregated loosely to the left, while the AD humanized ex-GF group segregated loosely to the right of component 1, with a little overlapping in the center (left, compare light green and dark green circles) (A). Within the serum dataset, the HC humanized ex-GF group segregated to the right, while the AD humanized ex-GF group segregated to the left of component 1, with some overlap in the center (middle, compare pink and maroon circles) (B). PCA analysis of brain dataset from GF/SPF and AD/HC inoculated ex-GF groups (C). Within the brain dataset, the GF group segregated away from the other groups, while the SPF, HC humanized ex-GF, and AD humanized ex-GF groups each segregated loosely throughout component 2 (right, compare light blue, dark blue, light purple, and dark purple circles).

(D-F) Differences in microbiome-related metabolites in feces (D), serum (E) and brain (F) from AD humanized ex-GF groups versus HC humanized ex-GF groups.

(G-I) Differences in carbohydrate and energy metabolites in feces (G), serum (H), and brain (I) from AD humanized ex-GF groups versus HC humanized ex-GF groups.

Red and green shaded cells indicate $P \leq 0.05$ (red indicates the fold change values are significantly higher for that comparison; green values significantly lower). Light red and light green shaded cells indicate $0.05 < P < 0.10$ (light red indicates the fold change values trend higher for that comparison; light green values trend lower).

A

Sub Pathway	Biochemical Name	Welch's t-tst	
		Fold of Change	AD humanized ex-GF HC humanized ex-GF
Phosphatidylethanolamine(PE)	1-palmitoyl-2-oleoyl-GPE(16:0/18:1)	2.21	5.64
	1-palmitoyl-2-linoleoyl-GPE(16:0/18:2)	2.21	2.21
	1-palmitoyl-2-arachidonoyl-GPE(16:0/20:4)	3.23	3.23
	1-stearoyl-linoleoyl-GPE(18:0/18:2)	2.28	2.28
Short Chain Fatty Acid	butyrate/isobutyrate (4:0)	0.46	0.46
	valerate (5:0)	0.87	0.87

C

Sub Pathway	Biochemical Name	Welch's t-tst	
		Fold of Change	AD humanized ex-GF HC humanized ex-GF
Dihydrospingomyelins	behenoyl dihydrospingomyelin(d18:0/22:0)	1.32	1.32
	spingomyelin(d18:0/18:0,d19:0/17:0)	1.24	1.24
	spingomyelin(d18:0/20:0,d16:0/22:0)	1.31	1.31
	behenoyl spingomyelin(d18:1/22:0)	1.21	1.21
Spingomyelins	tricosanyl spingomyelin(d18:1/23:0)	1.16	1.16
	liganoceroyl spingomyelin(d18:1/24:0)	1.20	1.20
	spingomyelin(d17:1/16:0,d18:1/15:0)	0.99	0.99
	spingomyelin(d18:2/16:0,d18:1/16:1)	1.02	1.02
	spingomyelin(d18:1/18:1,d18:2/18:0)	1.03	1.03
	spingomyelin(d18:1/19:0,d19:1/18:0)	1.15	1.15
Eicosanoid	spingomyelin(d18:1/20:0,d16:1/22:0)	1.18	1.18
	spingomyelin(d18:2/24:1,d18:1/24:2)	1.12	1.12
	Prostaglandin F2alpha	1.14	1.14
	12-HHTRE	1.10	1.10

D

Sub Pathway	Biochemical Name	Welch's t-tst	
		Fold of Change	AD humanized ex-GF HC humanized ex-GF
Urea Cycle; Arginine and Proline Metabolism	argininosuccinate	2.33	2.33
	ornithine	4.17	4.17
	3-amino-2-piperidone	1.85	1.85
	citulline	1.75	1.75
	dimethylarginine(SDMA+ADMA)	1.46	1.46
	N-delta-acetylornithine	1.34	1.34
	N-alpha-acetylornithine	3.55	3.55
	argininate	2.93	2.93

E

Sub Pathway	Biochemical Name	Welch's t-tst	
		Fold of Change	AD humanized ex-GF HC humanized ex-GF
Urea Cycle; Arginine and Proline Metabolism	arginine	1.37	1.37
	2-oxo arginine	1.46	1.46
	homocitrulline	0.84	0.84
	N-acetylproline	1.83	1.83
	pro-hydroxy-pro	0.71	0.71
	argininate	1.66	1.66

F

Sub Pathway	Biochemical Name	Welch's t-tst	
		Fold of Change	AD humanized ex-GF HC humanized ex-GF
Urea Cycle; Arginine and Proline Metabolism	ornithine	1.35	1.35
	2-oxo arginine	1.12	1.12
	homocitrulline	0.71	0.71
	proline	1.10	1.10
	N-delta-acetylornithine	0.90	0.90

B

Sub Pathway	Biochemical Name	Welch's t-tst	
		Fold of Change	AD humanized ex-GF HC humanized ex-GF
Long Chain Monounsaturated Fatty Acid	myristoleate(14:1n5)	0.38	0.38
	palmitoleate(16:1n7)	0.36	0.36
	10-heptadecenoate(17:1n7)	0.45	0.45
	oleate/vaccenate(18:1)	0.51	0.51
Long Chain polyunsaturated Fatty Acid (n3 or n6)	10-nonadecenoate(19:1n9)	0.52	0.52
	tetradecatrienoate(14:2)	0.45	0.45
	heneicosapentaenoate(21:5n3)	0.57	0.57
	docosapentaenoate(n3 DPA;22:5n3)	0.57	0.57
	hexadecatrienoate(16:2n6)	0.44	0.44
	dihomo-linoleate(20:2n6)	0.58	0.58
	dihomo-linolenate(20:3n3 or n6)	0.60	0.60
	docosapentaenoate(n6 DPA;22:5n6)	0.58	0.58
Fatty Acid Metabolism(Acyl Carnitine - Long Chain Saturated)	docosadienoate(22:2n6)	0.55	0.55
	myristoylcarnitine(C14)	0.48	0.48
	pentadecanoylcarnitine(C15)	0.44	0.44
	palmitoylcarnitine(C16)	0.45	0.45
Fatty Acid Metabolism(Acyl Carnitine - Monounsaturated)	margaroylcarnitine(C17)	0.52	0.52
	myristoylcarnitine(C14:1)	0.45	0.45
	palmitoleoylcarnitine(C16:1)	0.29	0.29
	oleoylcarnitine(C18:1)	0.35	0.35
Fatty Acid Metabolism(Acyl Carnitine - Polyunsaturated)	eicosenoylcarnitine(C20:1)	0.40	0.40
	linoleoylcarnitine(C18:2)	0.40	0.40
	linoleoylcarnitine(C18:3)	0.42	0.42
	dihomo-linoleoylcarnitine(C20:2)	0.39	0.39
	arachidonoylcarnitine(C20:4)	0.64	0.64
	dihomo-linoleoylcarnitine(C20:3n3 or 6)	0.53	0.53
Fatty Acid Metabolism(Acyl Choline)	docosahexaenoylcarnitine(C22:6)	0.50	0.50
	palmitoylcholine	0.30	0.30
	oleoylcholine	0.36	0.36
	stearoylcholine	0.31	0.31
Short Chain Fatty Acid	butyrate/isobutyrate (4:0)	0.65	0.65
Eicosanoid	thromboxane B2	1.13	1.13
	12-HHTRE	1.31	1.31

G

Sub Pathway	Biochemical Name	Welch's t-tst	
		Fold of Change	AD humanized ex-GF HC humanized ex-GF
Methionine, Cysteine, SAM and Taurine Metabolism	N-acetylmethionine	1.61	1.61
	S-adenosylhomocysteine(SAH)	2.97	2.97
	cysteine s-sulfate	1.88	1.88
Glutathione Metabolism	S-cystoproline	0.66	0.66
	ophthalate	1.41	1.41
Gamma-glutamyl Amino Acid	gamma-glutamylleucine	1.29	1.29
	gamma-glutamyl-alpha-lysine	1.24	1.24
	gamma-glutamylmethionine	2.89	2.89
	gamma-glutamylphenylalanine	1.39	1.39
	gamma-glutamylthreonine	1.45	1.45
	gamma-glutamylcitrulline	2.03	2.03
gamma-glutamyl-2-aminobutyrate	2.03	2.03	

H

Sub Pathway	Biochemical Name	Welch's t-tst	
		Fold of Change	AD humanized ex-GF HC humanized ex-GF
Methionine, Cysteine, SAM and Taurine Metabolism	S-adenosylhomocysteine(SAH)	1.11	1.11
	cysteine	0.98	0.98
	hypotaurine	1.06	1.06
	N-acetyltaurine	0.99	0.99
Glutathione Metabolism	cyano-alanine	1.09	1.09
	glutathione, reduced(GSH)	1.00	1.00
	glutathione, oxidized(GSSG)	0.96	0.96
	cysteinylglycine	0.99	0.99
	2-hydroxybutyrate/2-hydroxyisobutyrate	0.99	0.99
	S-(1,2-dicarboxyethyl)glutathione	1.10	1.10
	4-hydroxy-noncral-glutathione	1.12	1.12
3'-dephospho-CoA-glutathione	0.97	0.97	
Gamma-glutamyl Amino Acid	gamma-glutamyl-epsilon-lysine	0.97	0.97
	gamma-glutamylphenylalanine	1.02	1.02

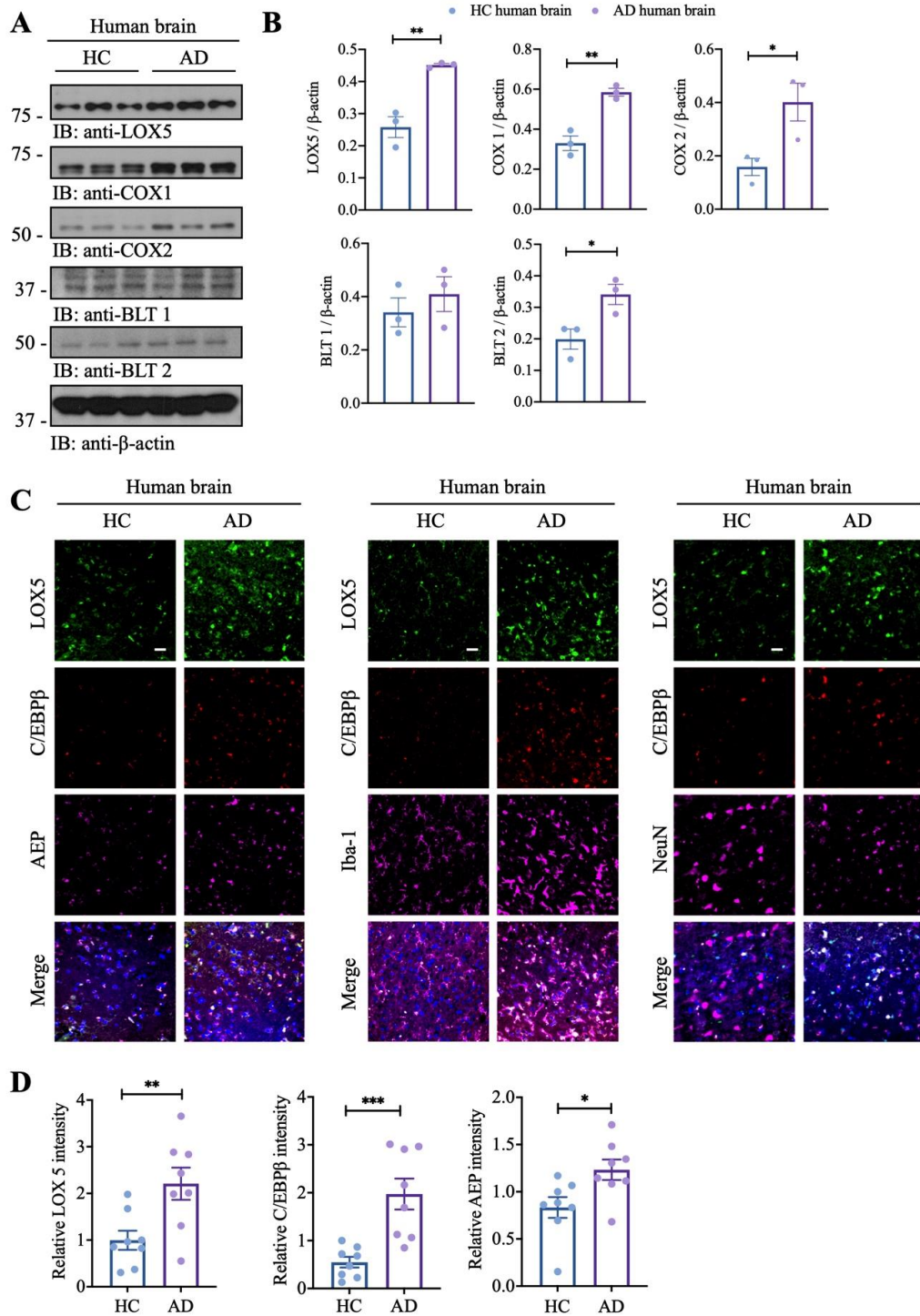
Supplementary Figure 11. Metabolomics analysis of the brains, serum samples and feces from AD humanized ex-GF 3xTg mice and HC humanized ex-GF 3xTg mice.

(A-C) Differences in lipid metabolism in feces (A), serum (B) and brain (C). The SCFAs, especially butyrate, were reduced in the feces and serum in AD humanized ex-GF 3xTg mice, whereas AA-associated metabolites including Thromboxane B2, Prostaglandin F2 α , 12-HHTrE were increased in the serum and the brain.

(D-F) Differences in arginine metabolism in feces (D), serum (E) and brain (F).

(G&H) Differences in oxidative stress metabolites in serum (G) and brain (H).

Red and green shaded cells indicate $P \leq 0.05$ (red indicates the fold change values are significantly higher for that comparison; green values significantly lower). Light red and light green shaded cells indicate $0.05 < P < 0.10$ (light red indicates the fold change values trend higher for that comparison; light green values trend lower).



Supplementary Figure 12. AD patient brains demonstrate enhanced AA-associated LOX/COX1/2 pathway, correlated with elevated C/EBP β /AEP signaling.

(A) Immunoblotting analysis of Arachidonic acid metabolism in the brain homogenates from AD patients and age-related healthy controls.

(B) Quantitative analysis of immunoblot. The bands of C/EBP β , LOX5, COX1, COX2, BLT1 and BLT2 were measured with Image J and normalized with β -actin. (n = 3 in each group. The expression of Arachidonic acid metabolism related protein increased in AD patients' brains. Data are shown as mean \pm SEM, *P<0.05, **P<0.01 compared with control, unpaired t tests).

(C) Immunofluorescent staining of LOX5, C/EBP β , AEP, Iba-1 and NeuN in the cortex region of the brains from Alzheimer's patients and age-related healthy controls. Scale bar: 20 μ m.

(D) Quantitative analysis of LOX5, C/EBP β and AEP positive cells. The fluorescence intensities of LOX5, C/EBP β and AEP positive cells in the brains of Alzheimer's patients were increased compared with age-related healthy controls. (n = 8 in each group, Data are shown as mean \pm SEM. *P< 0.05, **P< 0.01, ***P< 0.001 compared with control, unpaired t tests)

Supplementary Table 1 Clinical files of the human feces donors

Sample ID	Age	Gender	Dementia Rating of 2	Antibiotics past 6 months	Hospitalized past 6 months	Taking PPI	Any Acid reducing medication	Atypical Antipsychotics	malnutrition indicator score	Clinical Frailty Score ≥ 7	5 or more daily medications	Medications
AD_1	85	F	Yes	No	No	No	No	No	2	Y	Y	gabapentin, acetaminophen, miralax, atenolol, aspirin, trazodone, namenda, escitalopram, milk of magnesia, lorazepam, miralax, loratadine, donepezil, ativan, calcium supplement, ativan
AD_2	85	F	Yes	No	No	No	No	No	2	Y	Y	Vitamin D with calcium, children's chewable multivitamin, docusate sodium, levothyroxine, senna, simvastatin, vitamin C, ferrous sulfate, polyethylene glycol,
AD_3	94	F	Yes	No	No	No	No	No	2	Y	Y	hydrochlorothiazide, lisinopril, metoprolol tartrate, miralax, senokot, timolol maleate, tylenol,
HC_1	91	F	No	No	No	No	No	No	2	Y	Y	Glucernia, Melatonin, Vitamin D, Glizipide, Celexa, Simvastatin, Levothyroxine, multivitamin, actulose maalox maximum strength,
HC_2	94	F	No	No	No	No	No	No	2	Y	Y	Calcitonin, citalopram, furosemide, feri max, guaifenesin, lisinopril, milk of magnesia, multivitamin, salopas, senna, prednisone, polyethylene glycol, acetaminophen, coumadin, Vitamin D3
HC_3	93	F	No	No	No	No	No	No	2	Y	Y	acetaminophen, aspirin, children's chewable multivitamin, Vitamin D, Flomax, Lasix, milk of magnesia, Neurontin, remeron, senokot